

Generalized power law model of blood flow in a stenosed bifurcated artery

Muhammad Sabaruddin Ahmad Jamali ^{a*}, Zuhaila Ismail ^b

Department of Mathematical Sciences, Faculty of Science, Universiti Teknologi Malaysia .
81310 Johor Bahru, Johor, Malaysia.

* Coressponding Author. E-mail: ^a sabaruddin94@gmail.com, ^b zuhaila@utm.my

Abstract. Stenosis is a blockage caused by atherosclerosis literally lead to serious circulatory complaints, by narrowing the vessel wall and causing an alternation in the flow structure which consequently reduced the fluid flow passing to the other organs and tissues. This study, the geometry of the bifurcated is considered with presence of stenosis at mother and daughter artery. The blood vessel is modelled as a two-dimensional (2D) rigid wall since the wall of a disease artery is reported to be less compliant. The blood will be assumed as incompressible, laminar, steady and characterized as the generalized power-law model. Simulation result is obtained by using COMSOL Multiphysics 5.2, a software based on the FEM to solve the problem. Results concerning the effect of different blood rheology and severity of stenosis on the streamlines pattern are discussed.

Keywords: Stenosis, Generalized Power Law, 3D, Bifurcated artery and COMSOL Multiphysics.

INTRODUCTION

Cardiovascular disease is common problem of the cardiovascular system where it is leading cause of death. Coronary artery disease is caused by atherosclerosis which happens due to stenosis which formed as a result of fatty substances, cholesterol, cellular waste products, and smooth muscle cells accumulation in the artery wall, Zaman (2015). This progressive abnormal narrowing can happen at daughter and mother lumen arteries. Stenosis is a localize plaque that cause the vessel wall narrowed and causing a alternations in the flow structure which consequently reduced the fluid flow passing to the other organs and tissues, Rabby *et.al* (2014).

Numerous previous studies on blood flow with stenosis in a single artery have been conducted such as Jahangiri et al (2015), Rabby et al (2015) and Sharma et al (2016). While in some investigations of stenosed bifurcation artery has been done by Bose and Banerjee (2015), Liza et al (2017), Srinivasacharya et al (2017). It has been suggested that the geometry of bifurcations, junctions and high curvatures of arteries are easily exposed to the atherosclerosis formation. The resulting of vortex and recirculation zone arises from the geometry itself and not from the pulsatility of the flow was reported by Stroud et al (2002). Lou et al (1993) investigate the effect of the non-Newtonian fluid on a pulsatile flow at the aortic bifurcation. They conclude that the large and medium bifurcated arteries might possibly lead to a major change in fluid loading on artery wall and exposed to either high or low shear stress. As the anatomical considerations, two different type of model has been considered in present study regarding to (Lefevre, 2000; Pan, 2011; Medina, 2006; Iakovou, 2005)

Furthermore, it has been confirmed that the Newtonian model is valid only when the shear rates is more than 100 s^{-1} (reciprocal seconds), which have a tendency to occur in big arteries only, (Pedley, 1980; Berger, 2000). Mostly, the non-Newtonian would be a more accurate depiction of blood flow in the arteries, especially for stenosed situations. The significant of Newtonian and non-Newtonian blood model such as Carreau model, Walburn-Schneck model, power law, Casson model and generalized power law model investigated by (Johnston, 2004). The result shows a low central velocity inlet and wall shear stress values of Newtonian model are lower than those of non-Newtonian. For high central velocity inlet and wall shear stress value of those Newtonian and non-Newtonian are nearly identical. However, the wall shear stress of Walburn-Schneck and Power Law are underestimate than those others. Again (Johnston, 2006), five non-Newtonian models of blood flow in human right coronary arteries

was compared in transient simulation and conclude that the generalized power law model approximates wall shear stress relatively small with the Newtonian model for low inlet velocities and in regions of low shear. Mandal (2007) considered generalized power law model to investigate the influence of the stenoses shape on the characteristics of blood flow. Sarifuddin (2009) studied the shear-thickening and shear-thinning of the generalized power law model in an artery with different kinds of stenosis; cosine, smooth-shaped constrictions and irregular without any body force. In this study, mainly focus on laminar flow through bifurcated artery with the effect of different location of stenosis on generalized power law model of blood flow in a stenosed bifurcated artery. The simulation result is obtained by using COMSOL Multiphysics 5.2, a software based on the FEM.

MODEL CONSTRUCTION

Different classifications of stenosis in artery to define considered lesions have been proposed by (Lefevre, 2000; Pan, 2011; Medina, 2006; Iakovou, 2005). TYPE I is model of geometry involving stenosis in the mother artery. TYPE II is a model of geometry involving stenosis in the mother artery and upper branch of bifurcation.

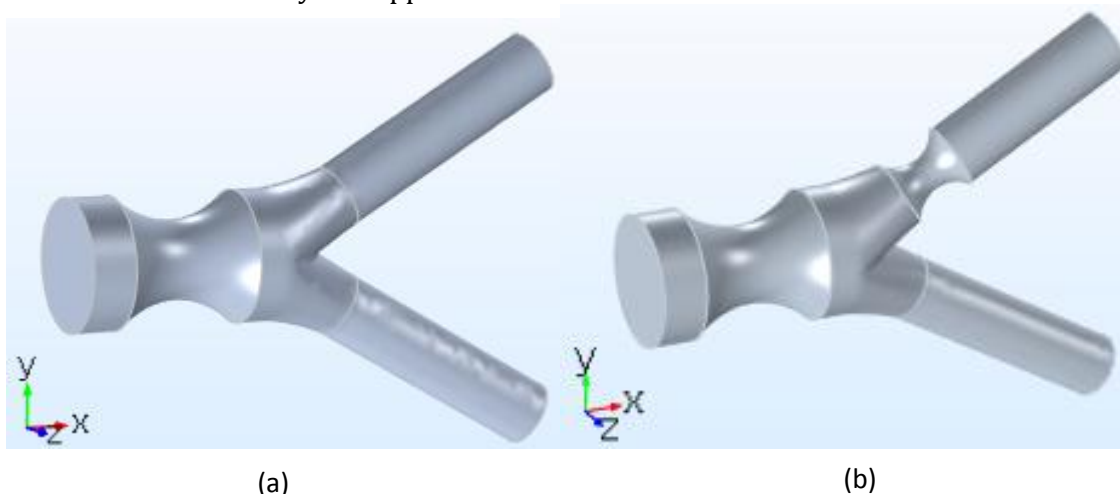


Figure 1. 3D geometry of the mild stenosis (a) at mother artery (TYPE I) and (b) at mother and upper branch bifurcation (TYPE II).

The Governing Equation

The streaming fluid representing blood in the arterial bifurcation is generally considered to be laminar and following the non-Newtonian Generalize Power law characteristic of fluid rheology. The governing equation of incompressible flow are given by

$$\frac{\partial u}{\partial x} + \frac{\partial v}{\partial y} + \frac{\partial w}{\partial z} = 0 \quad (1)$$

$$\rho \left(u \frac{\partial u}{\partial x} + v \frac{\partial u}{\partial y} + w \frac{\partial u}{\partial z} \right) = -\frac{\partial p}{\partial x} + \left(\frac{\partial \tau_{xx}}{\partial x} + \frac{\partial \tau_{yx}}{\partial y} + \frac{\partial \tau_{zx}}{\partial z} \right) \quad (2)$$

$$\rho \left(u \frac{\partial v}{\partial x} + v \frac{\partial v}{\partial y} + w \frac{\partial v}{\partial z} \right) = -\frac{\partial p}{\partial y} + \left(\frac{\partial \tau_{xy}}{\partial x} + \frac{\partial \tau_{yy}}{\partial y} + \frac{\partial \tau_{zy}}{\partial z} \right) \quad (3)$$

$$\rho \left(u \frac{\partial w}{\partial x} + v \frac{\partial w}{\partial y} + w \frac{\partial w}{\partial z} \right) = -\frac{\partial p}{\partial z} + \left(\frac{\partial \tau_{xz}}{\partial x} + \frac{\partial \tau_{yz}}{\partial y} + \frac{\partial \tau_{zz}}{\partial z} \right) \quad (4)$$

$$\bar{\tau} = - \left\{ m \left| \sqrt{\frac{1}{2} (\underline{\Delta} : \underline{\Delta})} \right|^{n-1} \right\} \underline{\Delta} \quad (5)$$

$$\tau_{xx} = -2 \left\{ m \left[\frac{1}{2} (\underline{\Delta} : \underline{\Delta}) \right]^{1/2} \right\}^{n-1} \left(\frac{\partial u}{\partial x} \right), \quad (6)$$

$$\tau_{yy} = -2 \left\{ m \left[\frac{1}{2} (\underline{\Delta} : \underline{\Delta}) \right]^{1/2} \right\}^{n-1} \left(\frac{\partial v}{\partial y} \right), \quad (7)$$

$$\tau_{zz} = -2 \left\{ m \left[\frac{1}{2} (\underline{\Delta} : \underline{\Delta}) \right]^{1/2} \right\}^{n-1} \left(\frac{\partial w}{\partial z} \right), \quad (8)$$

$$\tau_{xy} = \tau_{yx} = - \left\{ m \left[\frac{1}{2} (\underline{\Delta} : \underline{\Delta}) \right]^{1/2} \right\}^{n-1} \left(\frac{\partial v}{\partial x} + \frac{\partial u}{\partial y} \right), \quad (9)$$

$$\tau_{yz} = \tau_{zy} = - \left\{ m \left[\frac{1}{2} (\underline{\Delta} : \underline{\Delta}) \right]^{1/2} \right\}^{n-1} \left(\frac{\partial w}{\partial z} + \frac{\partial v}{\partial y} \right), \quad (10)$$

$$\tau_{zx} = \tau_{xz} = - \left\{ m \left[\frac{1}{2} (\underline{\Delta} : \underline{\Delta}) \right]^{1/2} \right\}^{n-1} \left(\frac{\partial w}{\partial x} + \frac{\partial u}{\partial z} \right). \quad (11)$$

where $\underline{\Delta}$ is the strain rate tensor and m is the fluid consistency coefficient and n is flow behaviour index. $\bar{\tau}$ is the stress tensor, u is the axial velocity, v is the radial velocity, y is the radial coordinate and x is axial coordinate. μ denotes the dynamic viscosity of blood, ρ is the density of blood, p is the pressure distribution acting on the surface.

Boundary Conditions

At the inlet, a parabolic velocity profile is imposed as:

$$u(x, y, z) = u_{\max} \left(1 - \left(\frac{y^2 + z^2}{x^2 + y^2} \right)^{\frac{n+1}{n}} \right), \quad v(x, y, z) = w(x, y, z) = 0, \quad \text{at } x = 0, -a < y < a \quad (12)$$

No-slip conditions along all the arterial walls:

$$u(x, y, z) = v(x, y, z) = w(x, y, z) = 0$$

A traction-free condition is applied at the outlet which can be stated as

$$(-p\mathbf{I} + \tau) \cdot \mathbf{n} = 0, \quad (13)$$

where \mathbf{n} represents a unit outward normal vector with the pressure point constraint, $p = 0$ being implemented at $x = 0$ and $y = 0.5$.

3D Computational Mesh

All computations were performed on a personal computer running 64 bit Windows 8 with speed of 1.70GHz and a RAM of 9.89GB. The geometry was drawn by means of the built-in CAD tools. Then the built-in meshing function was used to generate unstructured triangular elements of the model. Several attempt of mesh are perform in COMSOL Multiphysics to ensure the results obtained were not depended on the mesh parameters, see Figure 2 and Figure 3. The number of domain elements and maximum velocity computed using COMSOL Multiphysics in present study are summarised in Table 1 and Table 2.

Based on the mesh dependency test demonstrated from Table 1 and Figure 4, maximum velocity in range between Mesh 2 and Mesh 3 for TYPE I are nearly identical with slightly different of 0.00002m/s with domain element 719672 and 752913 respectively. Followed with TYPE II, maximum velocity in range between Mesh 3 and Mesh 4 are nearly identical with 0.00002 m/s with domain element 792489 and 866232 respectively. In order

to reduce computational time, mesh 2 and mesh 3 for TYPE I and YPE II respectively, is selected in order to provide a satisfactory solution to our problem.

Table 1. Mesh parameters for TYPE I and TYPE II.

Model	Parameter	Domain elements	Maximum velocity (m/s)
TYPE I	Mesh 1	604930	0.23586
	Mesh 2	719672	0.23598
	Mesh 3	752913	0.23600
	Mesh 4	865680	0.23634
TYPE II	Mesh 1	653346	0.40899
	Mesh 2	710968	0.40795
	Mesh 3	792489	0.40959
	Mesh 4	866232	0.40961

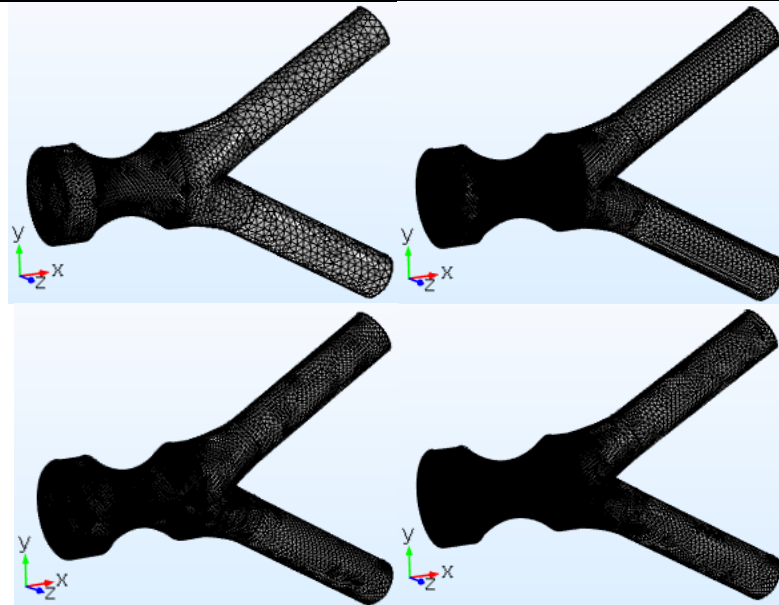


Figure 2. Different unstructured triangular mesh elements.

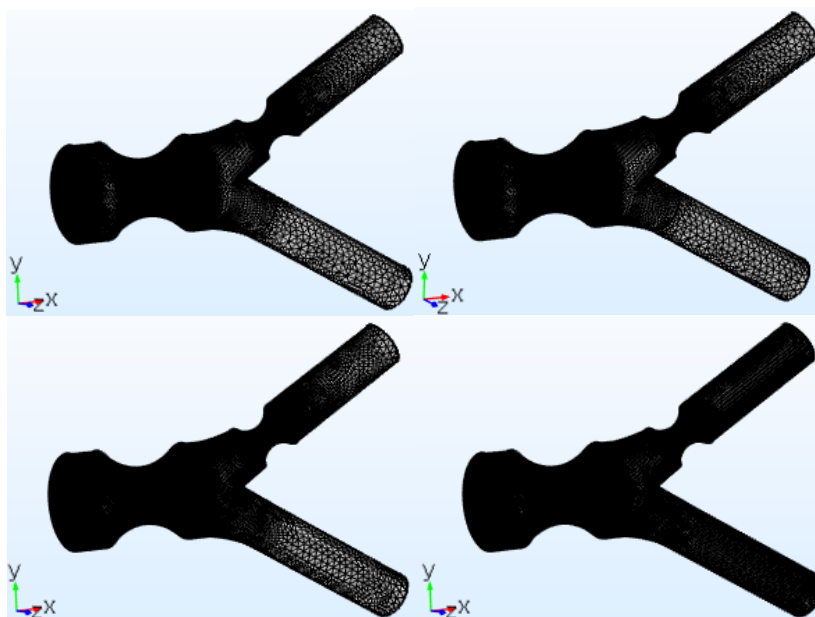
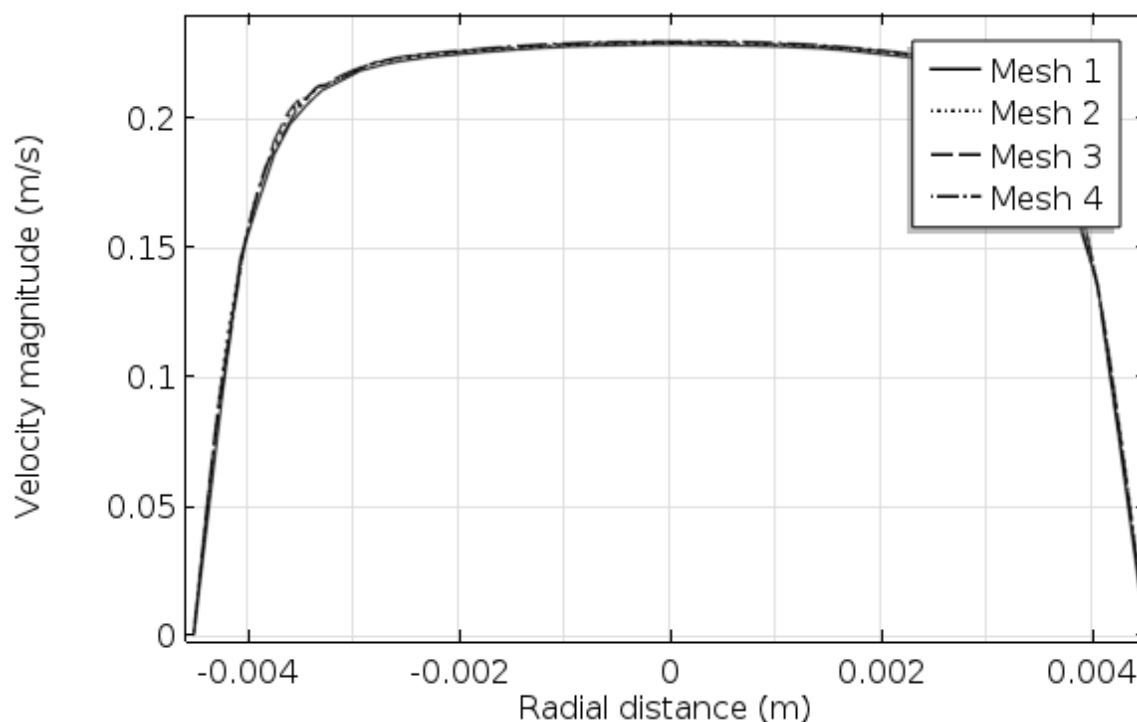
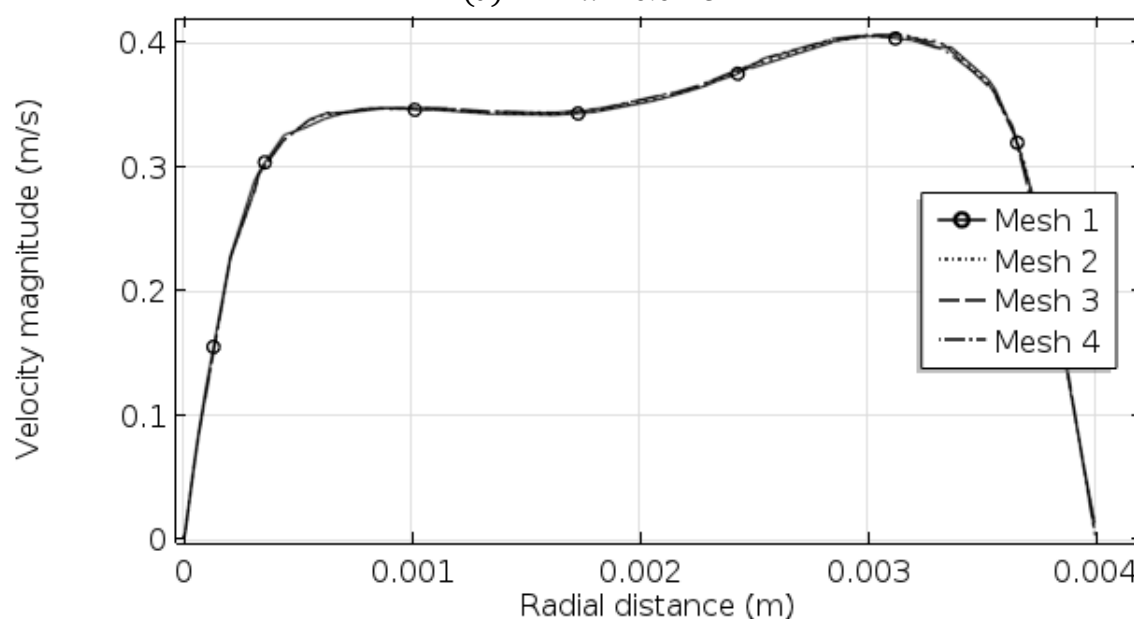


Figure 3. Different unstructured triangular mesh elements.



(a) $x = 0.0125$ m



(b) $x = 0.0350$ m

Figure 4. The axial velocity of 3D geometry for, a) TYPE I, and b) TYPE II

The Constriction of Stenosis

The occlusion is determined by the total blocked of the cross sectional where commonly defined as the 'throat' or constriction of the blockage. Referring Figure 6.5, the initial radius of the mother artery, $a = 0.0075$. Let $\pi = 0.4a$ and $\pi = 0.55a$ are the positive constant controlling the degree of stenosis constriction for both geometry TYPE I and TYPE II.

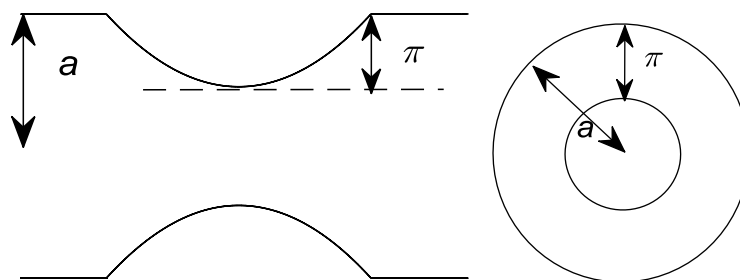


Figure 5: The geometry showing the degree of constriction at mother artery.

Model Validation

For the purpose of mesh dependency test and validation, geometry is used and constructed based on model proposed by Chakravarty (1995) and Zain (2017). Let (x, y) be the coordinates of a material point.

$$R_1(x) = \begin{cases} a, & 0 \leq x \leq d, \quad d + l_0 \leq x \leq x_1 \\ a - \frac{4\tau_m}{l_0^2} (l_0(x-d) - (x-d)^2), & d \leq x \leq d + l_0 \\ a + r_0 - \sqrt{r_0^2 - (x-x_1)^2}, & x_1 \leq x \leq x_2 \\ 2r_1 \sec \beta + (x-x_2) \tan \beta, & x_2 \leq x \leq x_{\max} - s \end{cases} \quad R_2(x) = \begin{cases} 0, & 0 \leq x \leq x_3 \\ \sqrt{r_0' - (x - (x_3 + r_0'))^2}, & x_3 \leq x \leq x_4 \\ r_0' \cos \beta + (x-x_4) \tan \beta, & x_4 \leq x \leq x_{\max} \end{cases}$$

where $R_1(x)$ and $R_2(x)$ represent the radii of the outer and inner wall, respectively. Meanwhile, a and r_1 are the respective radii of the mother and daughter artery. r_0 and r_0' are the radii of curvature for the lateral junction and the flow divider, respectively. Whereas, l_0 is the length of the stenosis at a distance d from the origin. Location of the onset and offset of the lateral junction are denoted by x_1 and x_2 , respectively. x_3 indicated as the apex, τ_m represents the maximum height of stenosis occur at $d + l_0/6$ and $d + 5l_0/6$ while β denote half of the bifurcation angle. Parameters involved in the above expressions may be given as

$$x_2 = x_1 + r_0 \sin \beta, \quad r_0 = (a - 2r_1 \sec \beta) / (\cos \beta - 1), \quad r_0' = (x_3 - x_2) \sin \beta / (1 - \sin \beta).$$

$$x_3 = x_2 + q, \quad s = 2r_1 \sin \beta, \quad x_4 = x_3 + r_0' (1 - \sin \beta).$$

The dimensional data for validation purpose has been made use from (Chakravarty, 1997; Zain, 2017):

$$a = 0.0075\text{m}, \quad l_0 = 0.015\text{m}, \quad d = 0.005\text{m},$$

$$x_{\max} = 0.06\text{m}, \quad x_1 = 0.025\text{m}, \quad \rho = 1050\text{kgm}^{-3}, \quad \mu = 0.0035\text{Pas}^{-1}, \quad \beta = 30^\circ, \quad q = 0.002\text{m}, \quad r_1 = 0.51a,$$

$$l_0 = 0.015\text{m}, \quad d = 0.005\text{m}, \quad x_{\max} = 0.06\text{m}, \quad x_1 = 0.025\text{m}.$$

Same procedure of meshing is applied in validation process to compute the 2D arterial bifurcation by considering blood as Newtonian. Several attempts of mesh have been made, see figure 6. The number of domain elements computed using COMSOL Multiphysics in present study are summarized in Table 3 followed together with its maximum velocity and coordinate. Table 2 consists of the respective maximum velocity obtained from COMSOL Multiphysics and Matlab from Zain (2017) together with its coordinate. From the outcome, both results obtained agreed well with each other with a very small difference recorded approximately 0.00043 m/s for the maximum velocity.

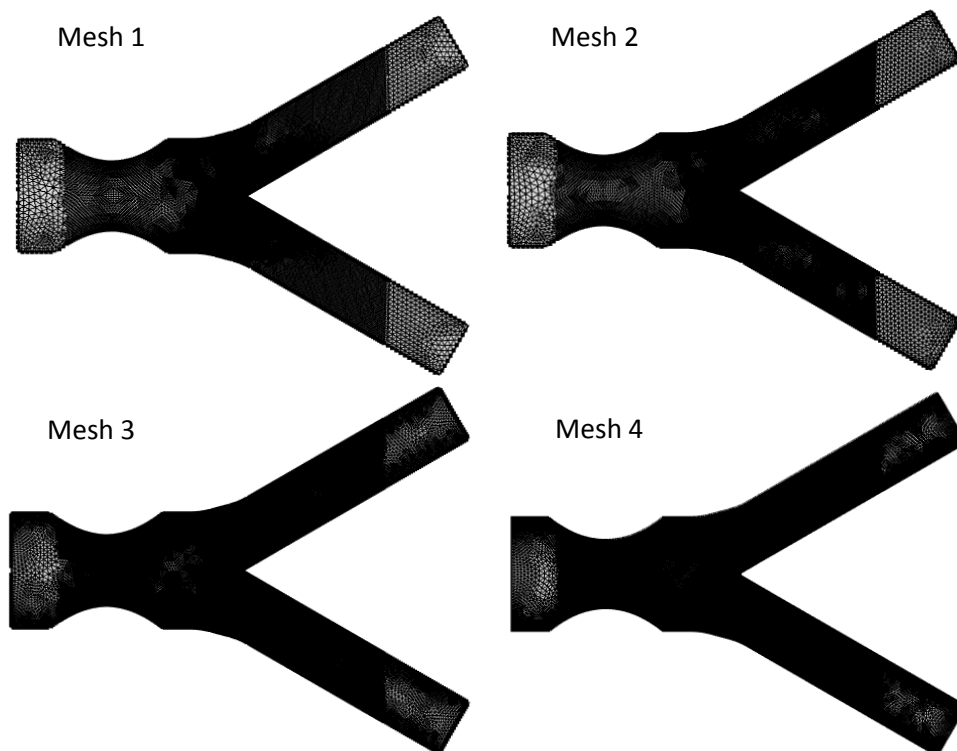


Figure 6. Different unstructured triangular mesh elements.

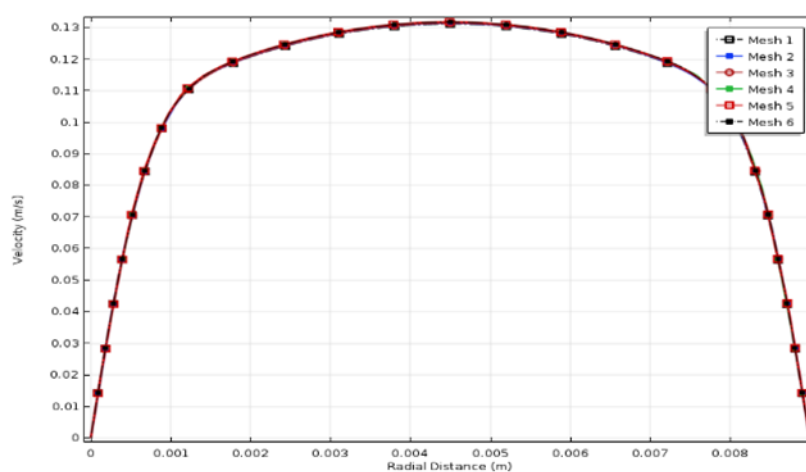


Figure 7. Velocity profiles with 40% of severity stenosis at $x = 0.0125m$.

Table 3. Comparison of maximum velocity and their coordinate

Software	Maximum velocity (m/s)	Coordinate (x, y)
COMSOL Multiphysics	0.13118	$(0.019154, 3.0259 \times 10^{-5})$
Matlab, Zain (2017)	0.13161	$(0.015, 2.6418 \times 10^{-5})$

RESULTS AND DISCUSSION

The governing equation (1)-(4) mentioned above were solved by using the commercial software package, COMSOL Multiphysics 5.2. Computational has been done on computer running 64-bit Window 8.1 with speed of 1.60GHz and RAM of 4.00GB. The numerical computations have been performed in order to visualize the streamlines with different type of blood rheology and severity of stenosis.

The influence of different type of blood rheology for TYPE I on the flow recirculation zones are illustrated on Figure 8 and Figure 9 for severity of 40% and 55% respectively. Overall, interesting to note that the recirculation zone appears at the offset of the stenosis near the upper and lower outer wall of artery. Clearly the reversed flow of the vortex reaches the edge of stenosis, it is unable to follow the curve of stenosis and to move away from the stenosis by changing its direction at the same time. To further visualize and understanding of the blood behavior, obviously that the recirculation zones are found to increase in sizes from shear-thinning $n=0.639$, Newtonian model $n=1$, to shear-thickening $n=1.2$ rheological. Among these three fluids, shear-thickening fluid moves faster and possesses a higher momentum. It is difficult for the same fluid layer to remain attached to suddenly changing geometry and expanding wall, thus exhibits a more predominant vortex along the outer wall. In fact, this result has good agreement with the experimental findings by Ahmed (1983) and the theoretical results in Middleman (1995) and Mustapha (2010). The increment of stenosis occlusion clearly give considerable effects on streaming blood where the size of recirculation became bigger as the degrees of occlusion increases. The flow reversal and recirculation zones are formed which might exposed an individual to a worsening effect of cardiovascular diseases.

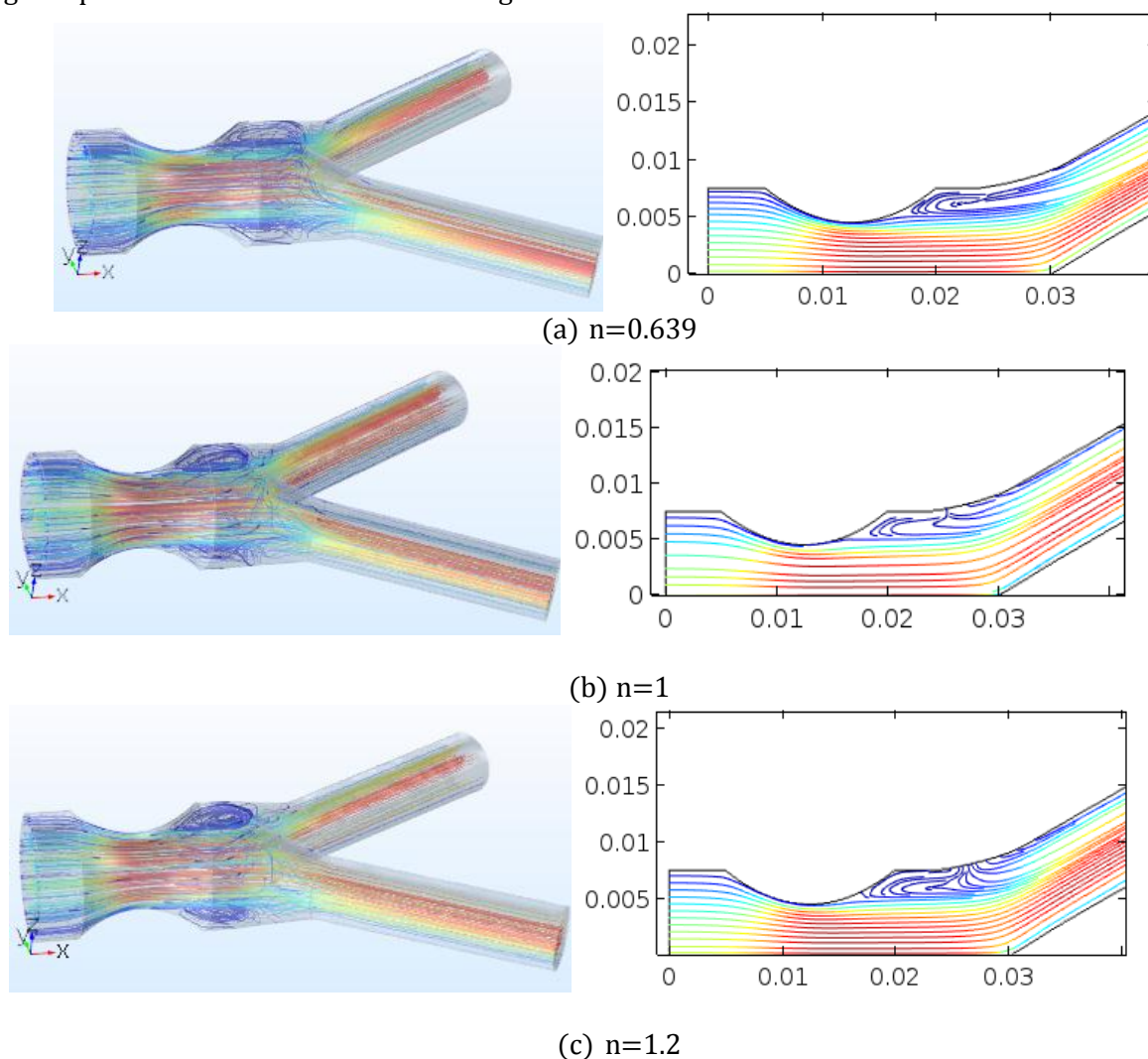


Figure 8. (a) 3D Streamline pattern for 40% occlusion of mother artery for different type of blood rheology.

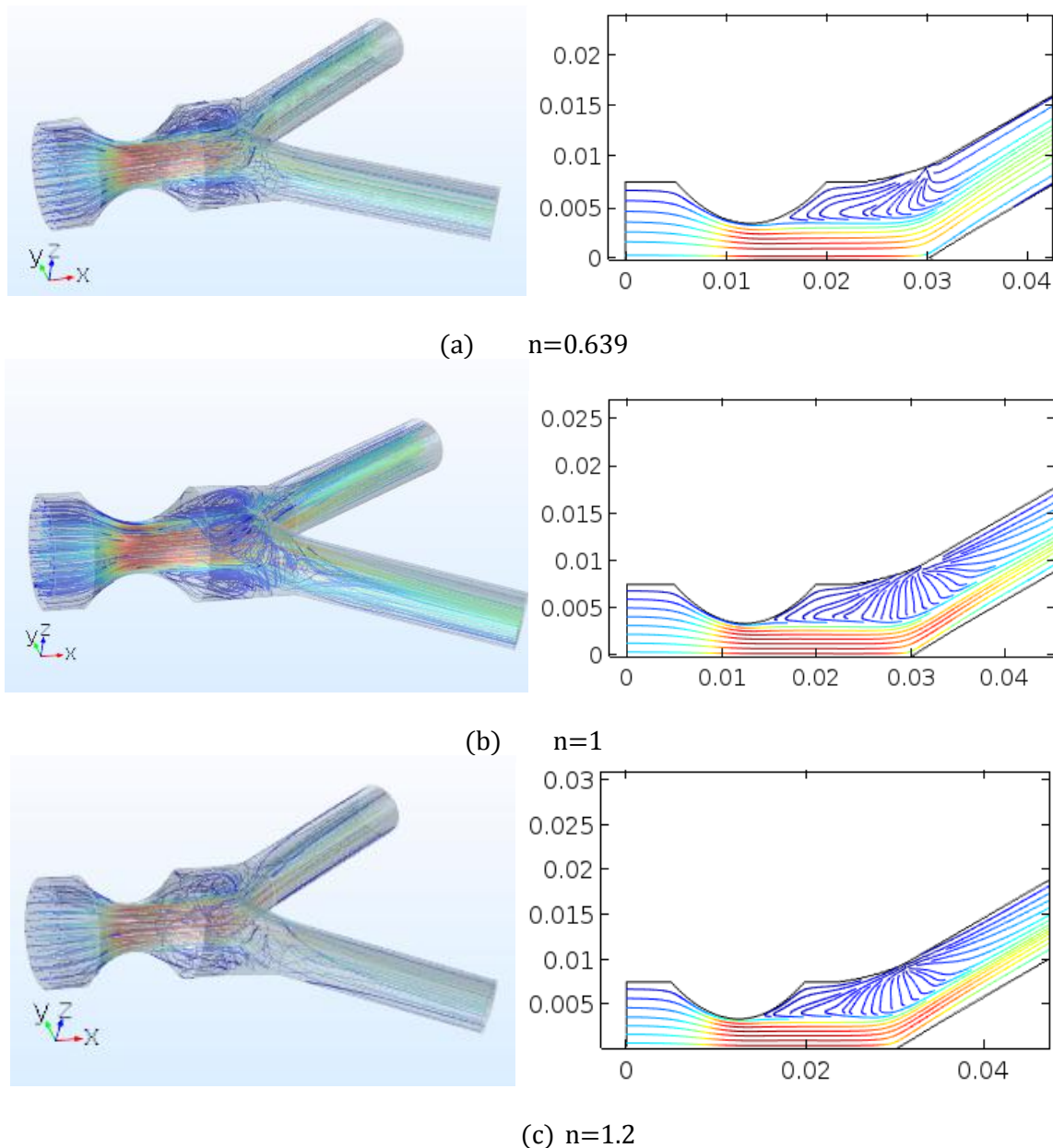


Figure 9. (a) 3D Streamline pattern for 55% degrees occlusion of mother artery for different type of blood rheology.

The influence of different type of blood rheology for TYPE II on the flow recirculation zones are illustrated on Figure 10 and Figure 11 for severity of 40% and 55% respectively. The reversal flow are formed at the offset of stenotic region in the mother artery and downstream of bifurcation and getting larger from shear-thinning $n = 0.639$, Newtonian model $n = 1$, to shear-thickening $n = 1.2$ rheological. In fact, with clearer picture as in Figure 10 and Figure 11, for each severity indicates that the recirculation zones are found to increase in sizes as the stenosis continue to enlarge. This increment cause the recirculation zone to elongate along the outer wall of daughter artery. Clearly from Figure 11 shows that a noticeable streamline pattern after pass through the throat of daughter artery, start to moving upward reaching the outer wall in which result of the big recirculation at the offset of the stenosis near the inner wall of artery . The recirculation near outer wall of bifurcated artery reducing in size and increasing the size near inner wall from shear-thinning $n = 0.639$, Newtonian model $n = 1$, to shear-thickening $n = 1.2$ rheological

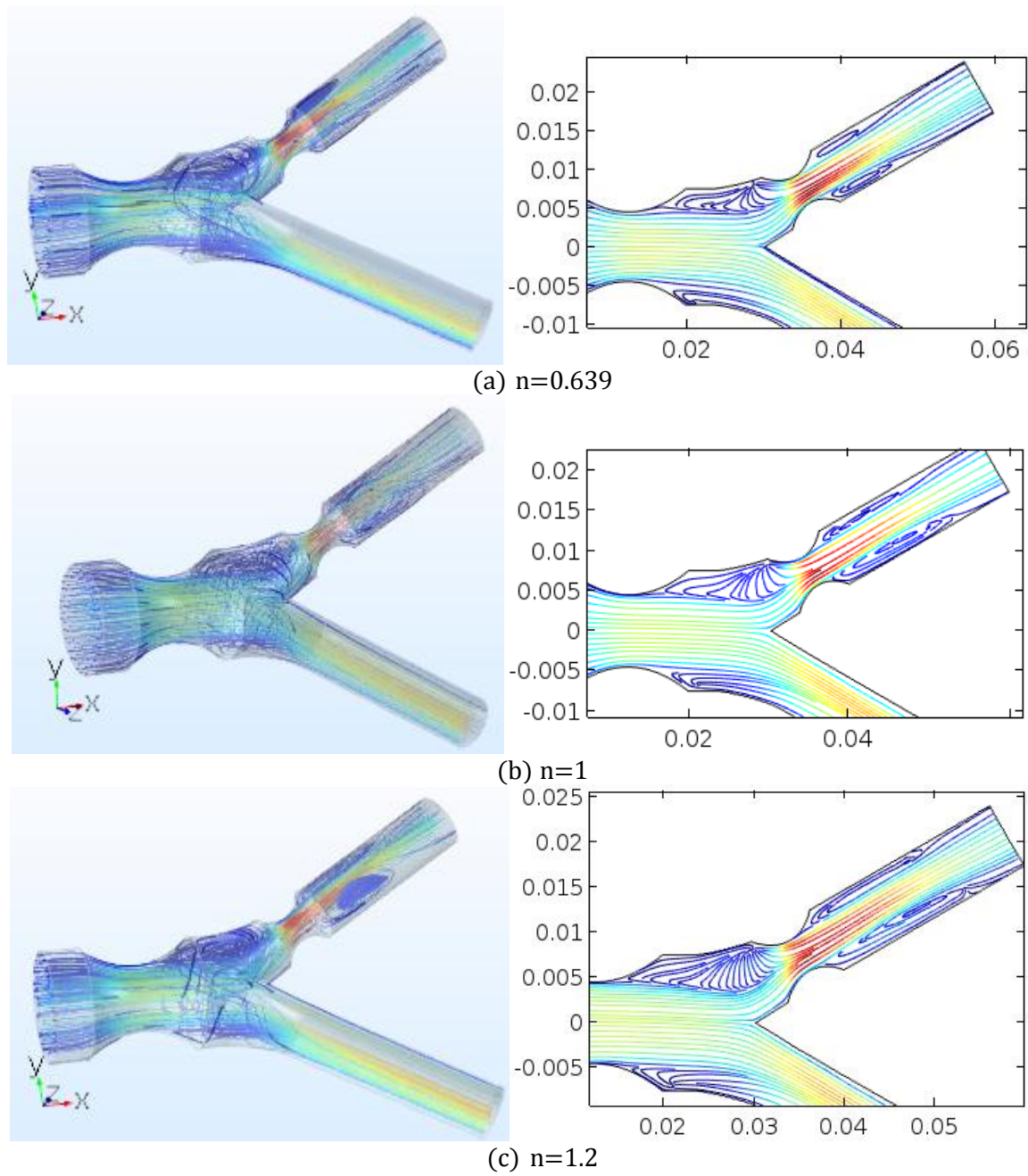
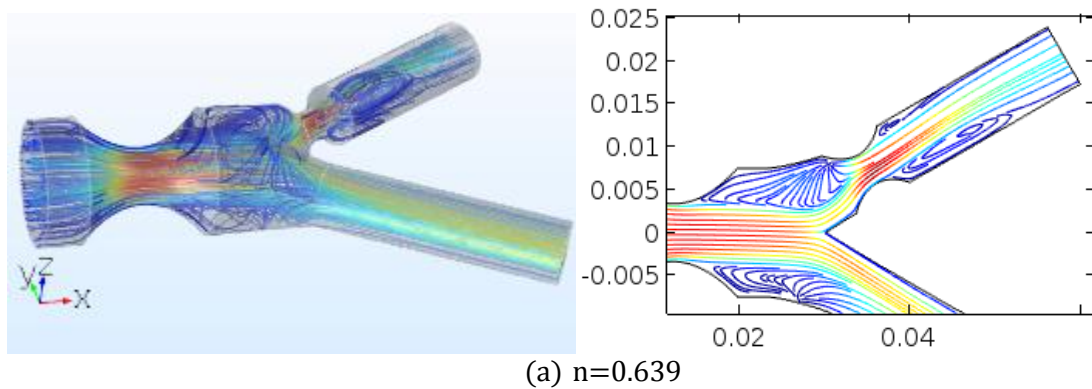


Figure 10. (a) 3D Streamline pattern for 40% occlusion of mother artery for different type of blood rheology.



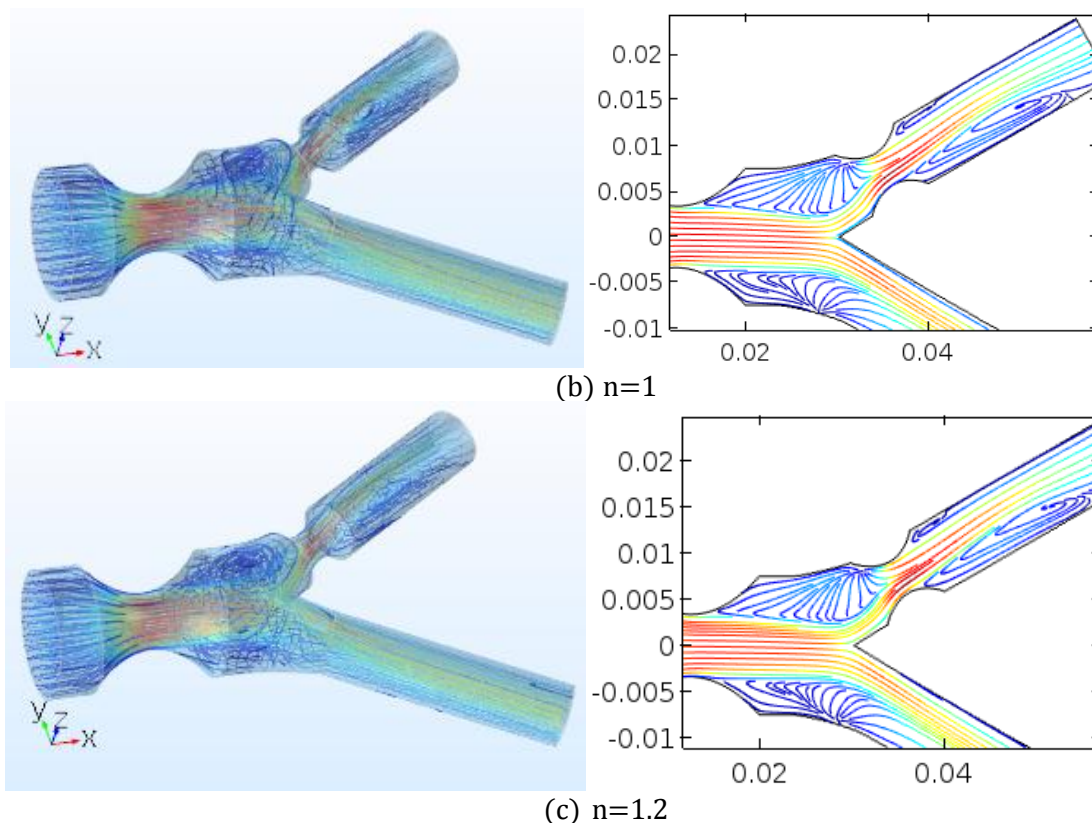


Figure 11. (a) 3D Streamline pattern for 55% occlusion of mother artery for different type of blood rheology.

CONCLUSION

In this work, the investigation of development three-dimensional mathematical model of steady flow in stenotic artery focused on the two type of models. The geometries proposed for TYPE I and TYPE II with each location of stenosis imposed in computational models have considerable impact on streamlines pattern. The flow of the blood has been governed by non-Newtonian of the streaming blood together with the effects of severity of stenosis. The non-Newtonian has been characterized by the generalized power-law model. The numerical computation is done using COMSOL Multiphysic 5.2. The effects of stenosis severity, different type of blood rheology and location of stenosis on streamlines pattern are approximated quantitatively. Based on the analyzation made, it can be observed that as the severity of the stenoses increases, the streamlines shown a abnormal behaviour where recirculation occur as the stenosis severity increases.

REFERENCES

- Ahmed, S.A., & Giddens, D.P. (1983). Velocity measurements in steady flow through axisymmetric stenoses at moderate Reynolds numbers. *Journal of biomechanics*, 16(7), pp.505-507.
- Berger, S.A., & Jou, L.D. (2000). Flows in stenotic vessels. *Annual Review of Fluid Mechanics*, 32(1), 347-382.
- Bose, S. & Banerjee, M. (2015) 'Magnetic particle capture for biomagnetic fluid flow in stenosed aortic bifurcation considering particle-fluid coupling', *Journal of Magnetism and Magnetic Materials*, 385(2015), 32-46.
- Iakovou, I., Ge, L., Colombo, A. (2005). Contemporary stent treatment of coronary bifurcations. *Journal of the American College of Cardiology* 46: 1447-1455.

- Jahangiri, M., Saghafian, M. & Sadeghi, M. R. (2015) 'Numerical study of turbulent pulsatile blood flow through stenosed artery using fluid-solid interaction', *Computational and Mathematical Methods in Medicine*, (515613), 1-10.
- Johnston, B.M, Johnston, P., Corney, S., and Kilpatrick, D. (2006). *Non-Newtonian Blood Flow in Human Right Coronary Arteries: Transient Simulations*. *Journal of Biomechanics*, 39(6), 1116-1128.
- Johnston, B.M., Johnston, P., Corney, S., & Kilpatrick, D. (2004). Non-newtonian blood flow in human right coronary arteries: steady state simulations. *Journal of Biomechanics*, 37(5), 709-720.
- Lefèvre T, Louvard Y, Morice MC, et al. (2000). Stenting of bifurcation lesions: classification, treatments, and results. *Catheterization and Cardiovascular Interventions* 49:274–283.
- Lou, Z. & Yang, W. -J. (1993) 'A computer simulation of the non-Newtonian blood flow at the aortic bifurcation', *J. Biomechanics*, 26(1), 37-49.
- Mandal, P.K., Chakravarty, S., & Mandal, A. (2007). Numerical study of the unsteady flow of non-newtonian fluid through differently shaped arteria stenoses. *International Journal of Computer Mathematics*, 84(7), 1059-1077.
- Medina, A., Lezo, J. S., & Pan, M. (2006). A new classification of coronary bifurcation lesions. *Rev Esp Cardiol* 59:183–184.
- Middleman, S., (1995). Modeling axisymmetric flows: dynamics of films, jets, and drops. Academic Press.
- Mustapha, N., Mandal, P.K., Johnston, P.R. & Amin, N., (2010). A numerical simulation of unsteady blood flow through multi-irregular arterial stenoses. *Applied Mathematical Modelling*, 34(6), pp.1559-1573.
- Pan, M., Medina, A., Lezo, J. S., et al. (2011). Coronary bifurcation lesions treated with simple approach (from the Cordoba & Las Palmas [CORPAL] Kiss Trial). *Am J Cardiol*, 107:1460 – 1465.
- Pedley, T. J. (1980). *The fluid mechanics of large blood vessels*. Cambridge University Press.
- Rabby, M.G., Shupti, S.P., & Molla, M.M. (2014). *Pulsatile Non-Newtonian Laminar Blood Flows through Arterial Double Stenoses*. *Journal of Fluids*. (757902): 1-13.
- Sarifuddin, Chakravarty, S., & Mandal, P.K. (2009). Effect of asymmetry and roughness of stenosis on non-newtonian flow past an arterial segment. *International Journal of Computational Methods*, 6 (3), 361-388
- Sharma, M. K., Nasha, V. & Sharma, P. R. (2016) 'A study for analyzing the effect of overlapping stenosis and dilatation on non-Newtonian blood flow in an inclined artery', *Journal of Biomedical Science and Engineering*, 9, 576-596.
- Srinivasacharya, D. & Rao, G. M. (2017) 'Micropolar fluid flow through a stenosed bifurcated artery', *Nonlinear Analysis : Modelling and Control*, 22(2), 147-159.
- Stroud, J. S., Berger, S. A. & Saloner, D. (2002) 'Numerical analysis of flow through a severely stenotic carotid artery bifurcation', *Journal of Biomechanical Engineering*, 124(1), 9-20
- Zain, L., & Ismail, Z. (2017) *Modelling of Newtonian blood flow through a bifurcated artery with the presence of an overlapping stenosis*. *Malaysian Journal of Fundamental and Applied Sciences Special Issue on Some Advances in Industrial and Applied Mathematics*, 304-309.
- Zaman, A., Ali, N., Sajid, M., & Hayat, T. (2015) Effects of Unsteadiness and non-Newtonian Rheology on Blood Flow through a Tapered Time-Variant Stenotic Artery. *AIP Advances*. 5(3): 0371291- 03712913.